Numerical analysis of photonic crystal fiber with chalcogenide core tellurite cladding composite microstructure*

Liu Shuo(刘 硕) and Li Shu-Guang(李曙光)†

Key Laboratory of Metastable Materials Science and Technology, College of Science, Yanshan University, Qinhuangdao 066004, *China*

(Received 17 August 2012; revised manuscript received 28 November 2012)

Kinds of photonic crystal fibers with chalcogenide core tellurite cladding composite microstructure are proposed. The multi-core photonic crystal fiber can reach the higher nonlinearity coefficient and the larger effective mode area. The small single-core photonic crystal fiber has a very high nonlinearity coefficient. At the wavelength $\lambda = 0.8$ μm, the nonlinearity coefficient can reach 31.37053 $W^{-1}\cdot m^{-1}$, at the wavelength $\lambda = 1.55$ μm, the nonlinearity coefficient is 11.19686 $W^{-1}\cdot m^{-1}$.

Keywords: multi-core photonic crystal fiber, effective mode area, nonlinearity coefficient, dispersion

PACS: 42.65.−k, 42.70.Mp, 42.81.−i **DOI:** 10.1088/1674-1056/22/7/074206

1. Introduction

The research based on photonic crystal fiber (PCF) has attracted great research interest recently. The large-mode-area and the high nonlinearity are two very important parameters of the PCF. Xiao *et al.*[1] reported the polarization-dependent dispersion and its impact on the optical parametric process in highly nonlinear microstructure fiber. Wang *et al.*[2] numerically demonstrated a high-nonlinearity single-mode holey fiber with flattened dispersion around the Ti–Za laser band at 800 nm. The nonlinearity coefficient was 170 $W^{-1}\cdot km^{-1}$ at 800 nm. Ebendorff-Heidepriem *et al.*[3] reported on the progress of bismuth oxide glass holey fibers for nonlinear device applications. The use of micron-scale core diameters had resulted in a very high nonlinearity of 1100 $W^{-1}\cdot km^{-1}$ at 1550 nm. Ademgil *et al.*[4] designed a simple index-guiding PCF with a nonlinearity coefficient of 49 $W^{-1}\cdot km^{-1}$ at the wavelength of 1.55 μm. Razzak *et al.*[5] proposed the microstructure optical fiber with the nonlinearity coefficient of the order 41 $W^{-1}\cdot km^{-1}$ at the wavelength of 1.55 μm. The wavelength-tunable high-energy ultra-short laser pulses can be generated from large-mode-area PCF.[6] Li *et al.*[7] reported on a quasi-three-level large-mode-area double-clad Yb-doped fiber laser. Limpert *et al.*[8] reported on a 2.3-m long air-clad ytterbium-doped large-mode-area PCF laser generating up to 80-W output power with a slope efficiency of 78%. Chen *et al.*[9] proposed a kind of all-solid large-mode-area microstructure-core optical fibers, numerical simulations demonstrated the possibility of single-mode guidance with the mode area extending to 11900 μm^2 at the wavelength of 1.55 μm. Vogel *et al.*[10] investigated a single-mode evanescently coupled multi-core fiber consisting of 19 hexagonally arranged cores, and reported on the fundamental mode with an effective area of 465 μm^2. Chen *et al.*[11] prepared the Yb^{3+}-doped double clad PCF with a large core of around 90 μm in diameter. The double clad PCF had a mode area of about 1330 μm^2. Zhang *et al.*[12] demonstrated a dissipative-soliton mode-locked laser based on Yb-doped single polarization large-mode-area PCF.

The nonlinearity coefficient is inversely proportional to the effective mode area. However, the multi-core PCF can make a balance between the high nonlinearity and the large mode area: it can have high nonlinearity and large-mode area. Hence, the multi-core PCF can achieve high power supercontinuum (SC) generation. Husakou *et al.*[13] showed that a frequency comb in the telecommunication region around 1550 nm can be generated by four-wave mixing in a doped multi-core PCF made from a highly nonlinear glass. Fang *et al.*[14] used seven-core multi-core PCF, which can generate 150-MW 110-fs pulses, to demonstrate the phase-locked amplification. She also experimentally studied a mode-locked fiber laser based on Yb-doped large-mode-area PCF operating in the all-normal dispersion regime.[15] Manili *et al.*[16] studied the process of SC spectrum generation in a birefringence multi-core PCF. Imamura *et al.*[17] successfully fabricated the multi-core fibers with a large effective area over 100 μm^2 and low micro bending loss. Zheng *et al.*[18] investigated the three-dimensional thermal properties of 18-core PCF lasers operated under natural convection.

Some research institutions have been studying the chalcogenide core tellurite cladding composite microstructure PCF. Xie *et al.*[19] proposed a chalcogenide-tellurite composite microstructure optical fiber, which has a flattened near-zero dispersion curve around 2.5 μm and has two dispersion wavelengths, and generated a wide SC spectrum covering from 1.8 μm to 6.0 μm by pumping pulses of energy below 10 pJ

*Supported by the National Natural Science Foundation of China (Grant Nos. 61178026 and 60978028), the Specialized Research Fund for the Doctoral Program of Higher Education of China (Grant No. 20091333110010), and the Natural Science Foundation of Hebei Province, China (Grant No. E2012203035).

†Corresponding author. E-mail: shuguangli@ysu.edu.cn

© 2013 Chinese Physical Society and IOP Publishing Ltd

per pulse. In 2010, Chaudhari *et al.*[20] simulated the optical amplification in the composite chalcogenide-tellurite microstructure fiber by a single wavelength pump or dual wavelength pumps. In 2012, Chaudhari *et al.*[21] presented the detailed design of a highly nonlinear chalcogenide core tellurite cladding composite microstructured fiber. It was observed that an SC spectrum of 20-dB bandwidth covering 0.80 μm–2.40 μm was generated by this composite microstructure fiber when 1.85-μm pump was used. The simulation results show that the bandwidth over which the calculated parametric gain was more than 10 dB was 1680 nm, ranging from 1.04 μm to 2.72 μm. Liao *et al.*[22] had studied in depth the chalcogenide-tellurite composite microstructure fiber, and fabricated the fiber successfully for the first time. The propagation loss at 1.55 μm was 18.3 dB/m, and the nonlinearity coefficient at 1.55 μm was 9.3 $m^{-1}\cdot W^{-1}$; they generated an SC spectrum of 20-dB bandwidth spanning 800 nm to 2400 nm using this fiber.

In this paper, three kinds of PCFs with chalcogenide core tellurite cladding composite microstructure are proposed. Comparing with the large single core PCF, the multi-core PCF has higher nonlinearity and a larger effective mode area. The small single core PCF has very high nonlinearity. We use the finite element method (FEM) to numerically simulate the characteristics of the PCFs.

2. Principle of operation

The new chalcogenide core tellurite cladding composite microstructure PCF structure is illustrated in Fig. 1. All the holes are arrayed in a regular octagon. The gray-hole diameter on the first and second rings are d_1 and d_2, respectively. The distance from the origin to the center of the gray-hole on the first ring is Λ_1, the distance from the origin to the center of the air-hole on the second ring is Λ_2, the pitch of the air-holes on the outer rings is Λ_3. Figure 1(a) shows the cross section of the multi-core PCF, figure 1(b) shows the cross section of the PCF1, the gray-hole diameter is $d_1 = 5.2$ μm, figure 1(c) shows the cross section of the PCF2, the gray-hole diameter $d_1 = 0.625$ μm.

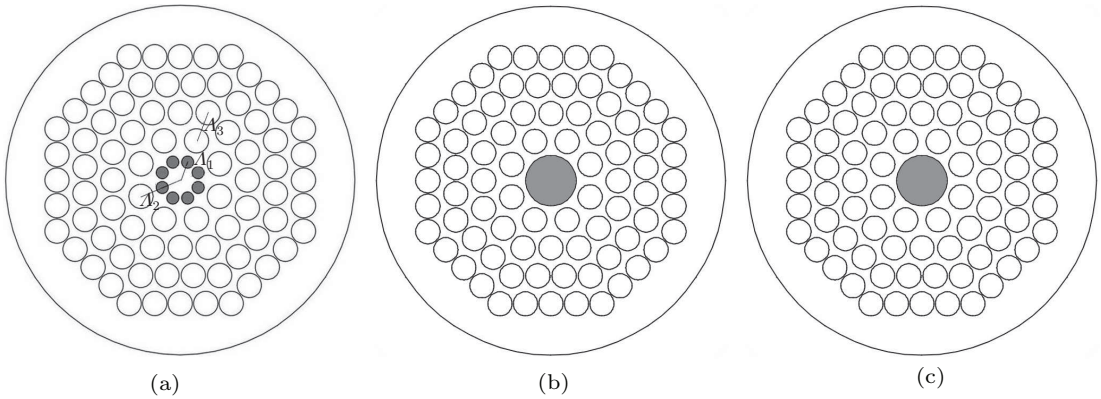


Fig. 1. Cross sections of the (a) multi-core PCF, (b) PCF1, and (c) PCF2.

The composition of the tellurite glass was $76.5TeO_2$–$6Bi_2O_3$–$11.5Li_2O$–$6ZnO$ (mol%). The refractive index can be obtained by the Sellmeier equation as follows:

$$n(\lambda) = \sqrt{1 + \frac{A\lambda^2}{\lambda^2 - D} + \frac{B\lambda^2}{\lambda^2 - E} + \frac{C\lambda^2}{\lambda^2 - F}}, \tag{1}$$

where $A = 1.67189$, $B = 1.34862$, $C = 0.62186$, $D = 0.0004665$ μm^2, $E = 0.0574608$ μm^2, $F = 46.72542736$ μm^2, and the wavelength λ is expressed in microns. The gray-holes are replaced with As_2S_3 chalcogenide glass and its refractive index can be obtained by the Sellmeier equation as follows:

$$n(\lambda) = \sqrt{1 + \frac{B_1\lambda^2}{\lambda^2 - C_1^2} + \frac{B_2\lambda^2}{\lambda^2 - C_2^2} + \frac{B_3\lambda^2}{\lambda^2 - C_3^2} + \frac{B_4\lambda^2}{\lambda^2 - C_4^2} + \frac{B_5\lambda^2}{\lambda^2 - C_5^2}}, \tag{2}$$

where $B_1 = 1.8983678$, $B_2 = 1.9222979$, $B_3 = 0.8765134$, $B_4 = 0.1188704$, $B_5 = 0.9569903$, $C_1^2 = 0.0225$ μm^2, $C_2^2 = 0.0625$ μm^2, $C_3^2 = 0.1225$ μm^2, $C_4^2 = 0.2025$ μm^2, $C_5^2 = 750$ μm^2, and the wavelength λ is expressed in microns. Figure 2 shows the refractive index value by varying the wavelength of the tellurite glass and the As_2S_3 chalcogenide glass. In the numerical simulation process, the refractive index with the variation of wavelength, so the material dispersion has been considered in our simulations.

The effective mode area $A_{\text{eff}}(\lambda)$ of the PCF can be calculated as

$$A_{\text{eff}}(\lambda) = \frac{(\iint F(x,y)^2 \mathrm{d}x\mathrm{d}y)^2}{\iint F(x,y)^4 \mathrm{d}x\mathrm{d}y}, \tag{3}$$

where $F(x,y)$ is the transverse electric field. The nonlinearity coefficient $\gamma(\lambda)$ of the chalcogenide core tellurite cladding composite microstructure PCF can be defined as[23]

$$\gamma(\lambda) = \frac{2\pi}{\lambda} \frac{\iint n_2(x,y) F(x,y)^4 \mathrm{d}x\mathrm{d}y}{(\iint F(x,y)^2 \mathrm{d}x\mathrm{d}y)^2}, \tag{4}$$

where n_2 is the nonlinearity index coefficient, n_2 of the As_2S_3 chalcogenide glass is 3.0×10^{-18} m^2/W,[24] n_2 of the tellurite glass is 5.9×10^{-19} m^2/W, n_2 of the air is 2.9×10^{-23} m^2/W.

The dispersion $D(\lambda)$ can be defined as[25]

$$D(\lambda) = -\frac{2\pi c}{\lambda^2}\beta_2 = -\frac{\lambda}{c}\frac{\mathrm{d}^2 n_{\mathrm{eff}}(\lambda)}{\mathrm{d}\lambda^2}, \tag{5}$$

where $n_{\mathrm{eff}}(\lambda)$ represents the effective index of the guided mode and can be calculated by using FEM.

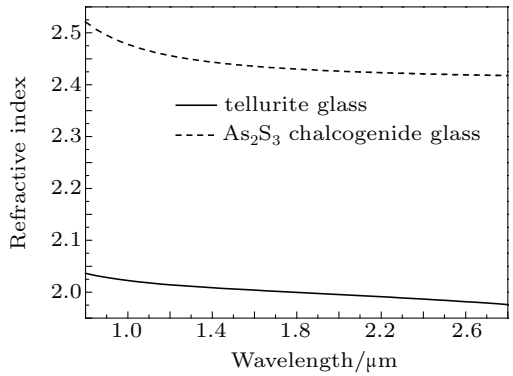


Fig. 2. The refractive index as a function of the wavelength.

3. Simulation results

3.1. Mode selection

As we all know the effective mode area of the single-core PCF is very small, and is easily broken by the high-power light. In order to support the high-power light, we design the multi-core PCF to enlarge the effective mode area. In this paper, we propose multi-core PCF with chalcogenide core tellurite cladding composite microstructure. When the light transmits in the multi-core PCF, the modes in these eight chalcogenide glass cores are coupled resulting in supermodes. The distribution of the electric field of each core[26]

$$E_m(x,y)\exp(\mathrm{i}\beta_m z). \tag{6}$$

The supermode $E(x,y,z)$ of the multi-core PCF can be approximated as a weighted superposition of the individual modes

$$E(x,y,z) = \sum_m A_m(z)E_m(x,y)\exp(\mathrm{i}\beta_m z), \quad m = 1,2,\ldots 8. \tag{7}$$

The mode of each core will be coupled. The coupling model equation can be expressed as

$$\frac{\mathrm{d}E(z)}{\mathrm{d}z} = CE(z), \tag{8}$$

where C is the coupling coefficient matrix, which is

$$\tilde{C} = \begin{pmatrix} \mathrm{i}s_1 & \mathrm{i}k_{12} & \mathrm{i}k_{13} & \mathrm{i}k_{14} & \mathrm{i}k_{15} & \mathrm{i}k_{16} & \mathrm{i}k_{17} & \mathrm{i}k_{18} \\ \mathrm{i}k_{21} & \mathrm{i}s_2 & \mathrm{i}k_{23} & \mathrm{i}k_{24} & \mathrm{i}k_{25} & \mathrm{i}k_{26} & \mathrm{i}k_{27} & \mathrm{i}k_{28} \\ \mathrm{i}k_{31} & \mathrm{i}k_{32} & \mathrm{i}s_3 & \mathrm{i}k_{34} & \mathrm{i}k_{35} & \mathrm{i}k_{36} & \mathrm{i}k_{37} & \mathrm{i}k_{38} \\ \mathrm{i}k_{41} & \mathrm{i}k_{42} & \mathrm{i}k_{43} & \mathrm{i}s_4 & \mathrm{i}k_{45} & \mathrm{i}k_{46} & \mathrm{i}k_{47} & \mathrm{i}k_{48} \\ \mathrm{i}k_{51} & \mathrm{i}k_{52} & \mathrm{i}k_{53} & \mathrm{i}k_{54} & \mathrm{i}s_5 & \mathrm{i}k_{56} & \mathrm{i}k_{57} & \mathrm{i}k_{58} \\ \mathrm{i}k_{61} & \mathrm{i}k_{62} & \mathrm{i}k_{63} & \mathrm{i}k_{64} & \mathrm{i}k_{65} & \mathrm{i}s_6 & \mathrm{i}k_{67} & \mathrm{i}k_{68} \\ \mathrm{i}k_{71} & \mathrm{i}k_{72} & \mathrm{i}k_{73} & \mathrm{i}k_{74} & \mathrm{i}k_{75} & \mathrm{i}k_{76} & \mathrm{i}s_7 & \mathrm{i}k_{78} \\ \mathrm{i}k_{81} & \mathrm{i}k_{82} & \mathrm{i}k_{83} & \mathrm{i}k_{84} & \mathrm{i}k_{85} & \mathrm{i}k_{86} & \mathrm{i}k_{87} & \mathrm{i}s_8 \end{pmatrix}, \tag{9}$$

where s_m is the propagation constant of the m-th individual cores, and k_{mn} is the coupling coefficient between the m-th and n-th cores. We define a propagating supermode as a field vector

$$E(z) = E(0)\exp(\mathrm{i}\beta z), \tag{10}$$

where β is the propagation constant of the supermode. Hence, we can obtain eight eigenvalues of supermodes.

To achieve the purpose of mode shaping, the propagation constant and coupling coefficient of PCF are changed by adjusting the PCF structure. By simulating with FEM, we can obtain the equal intensity eight Gauss beams from the multi-core PCF with proper parameters: $d_1 = 0.625$ μm, $d_2 = 1.25$ μm, $\Lambda_1 = 2$ μm, $\Lambda_2 = 4.375$ μm, and $\Lambda_3 = 3.125$ μm. Figure 3 shows the supermode in multi-core PCF. The electric field distribution of the supermodes is indicated by the red arrow. Each supermode has its own distinctive intensity distribution and diffraction property, but only the in-phase supermode has a Gaussian-shaped far-field intensity distribution.[27] Figure 4 shows the far-field distribution of the in-phase supermode. Therefore, in this paper, we only consider the in-phase supermode.

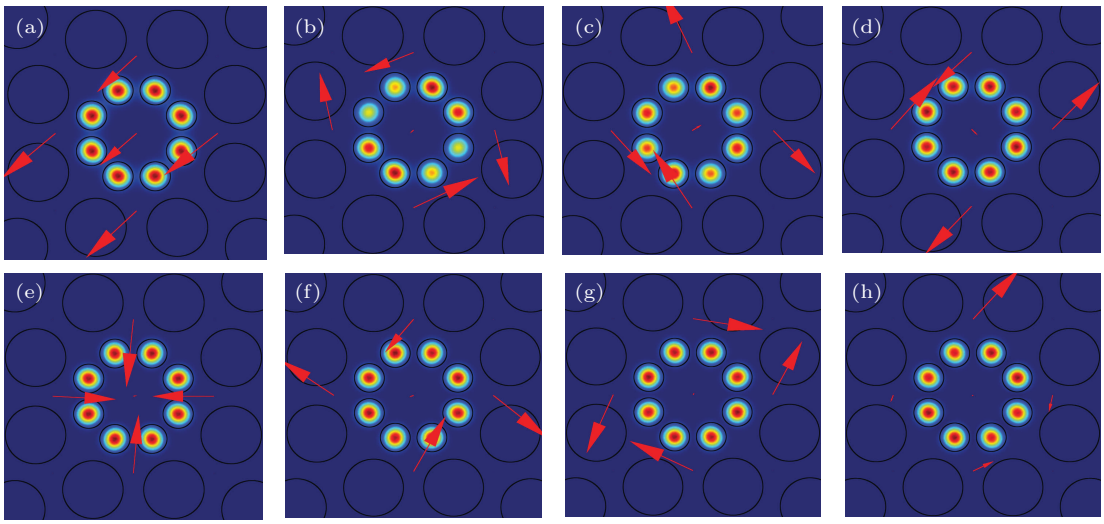


Fig. 3. Distributions of eight supermodes in multi-core PCF at the wavelength of 1.55 μm.

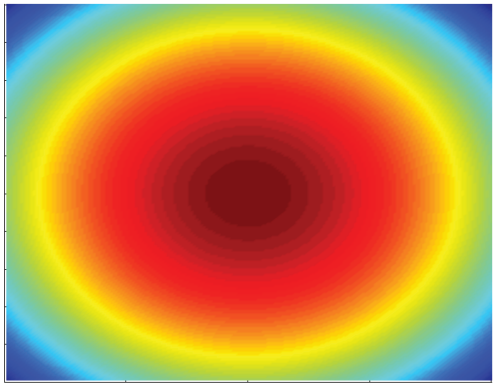


Fig. 4. Far-field distribution of the in-phase supermode.

3.2. Large effective mode area and highly nonlinear multi-core PCF

Figure 5 shows the effective mode area value by varying wavelengths of the multi-core PCF and the PCF1. It shows that the effective mode area increases with the wavelength. At the wavelengths of 0.8 μm and 1.55 μm, the multi-core PCF has large effective mode area. The effective mode areas of the multi-core PCF are 5.98443 μm^2 at the wavelength $\lambda = 0.8$ μm and 9.19733 μm^2 at the wavelength $\lambda = 1.55$ μm.

Figure 6 shows the nonlinearity coefficient values with different wavelengths. It shows that the nonlinearity coefficient decreases with the increase of wavelength. At the wavelengths of 0.8 μm and 1.55 μm, the multi-core PCF has larger nonlinearity coefficients than that of PCF1. The nonlinearity coefficients of the multi-core PCF are 3.93593 $W^{-1}\cdot m^{-1}$ at the wavelength $\lambda = 0.8$ μm and 1.30134 $W^{-1}\cdot m^{-1}$ at the wavelength $\lambda = 1.55$ μm.

The above discussions indicate that the multi-core PCF with chalcogenide core tellurite cladding composite microstructure can have large effective mode areas and high nonlinearity coefficients at the wavelengths of 0.8 μm and 1.55 μm. Compared with the single-core PCF, the advantages of multi-core PCF are the higher nonlinearity coefficient and larger effective mode area. In our proposed design, each small chalcogenide glass core can have high nonlinearity. When they combine together, we can obtain a large effective mode. Therefore, we proposed that the multi-core PCF can support high-power light transmission and achieve high nonlinearity requirement.

Figure 7 shows the chromatic dispersion values by varying of the multi-core PCF, PCF1 and PCF2. The PCFs with chalcogenide core tellurite cladding composite microstructure have large negative dispersions in wavelengths ranging from 0.8 μm to 1.55 μm. The zero dispersion wavelengths (ZDWs) of the multi-core PCF is 2.57 μm.

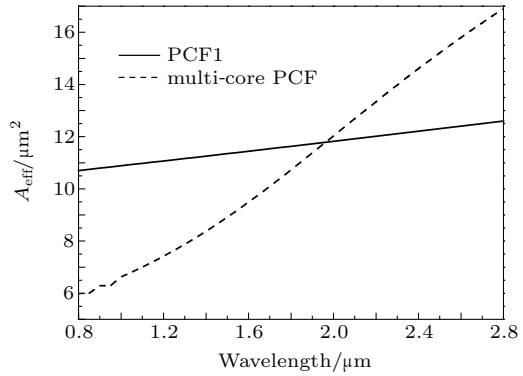


Fig. 5. The effective mode area A_{eff} as a function of the wavelength.

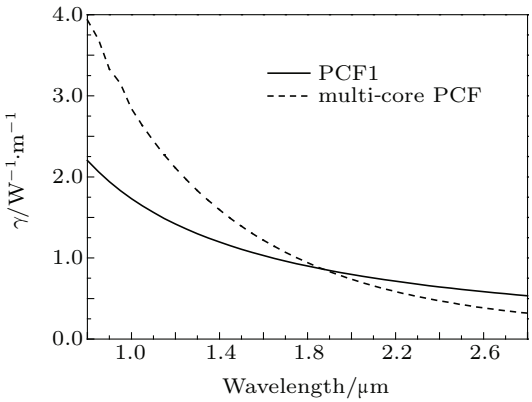


Fig. 6. The nonlinearity coefficient γ as a function of the wavelength.

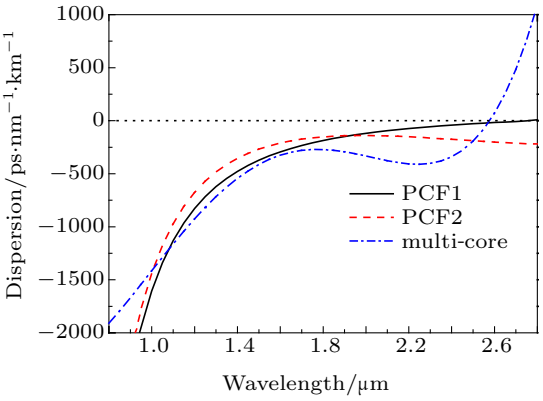


Fig. 7. The total chromatic dispersion versus the wavelength.

3.3. Highly nonlinear PCF

In this paper, we present that the PCF with chalcogenide core tellurite cladding composite microstructure has a high nonlinearity refractive index. Figure 8 shows the effective mode area and the nonlinearity coefficient value versus the wavelength in PCF2. From Fig. 8, we can see that the PCF2 has a very small effective mode area. The effective mode areas of the PCF2 are 0.75086 μm^2 at the wavelength $\lambda = 0.8$ μm and 1.0764 μm^2 at the wavelength $\lambda = 1.55$ μm. The nonlinearity coefficient is inversely proportional to the effective mode area. Hence, the PCF2 can have very high nonlinearity coefficients. At the wavelength $\lambda = 0.8$ μm,

the nonlinearity coefficient can reach 31.37053 $W^{-1}\cdot m^{-1}$, at the wavelength $\lambda = 1.55$ μm, the nonlinearity coefficient is 11.19686 $W^{-1}\cdot m^{-1}$. Therefore, the PCF2 with high nonlinearity can be used in optical soliton communication, high-power pulse compression, optical device fabrication, as well as the frequency changes.

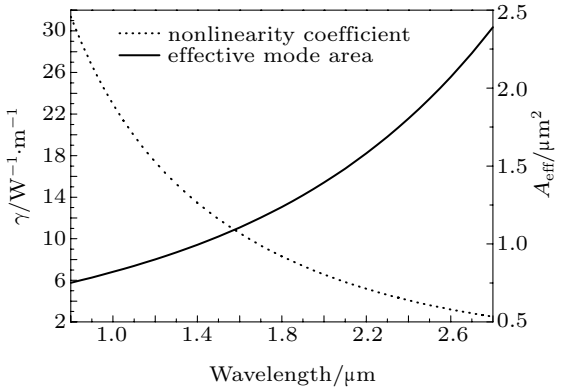


Fig. 8. The nonlinearity coefficient γ and the effective mode area $A_{\rm eff}$ as functions of the wavelength in PCF2.

4. Conclusion

This paper presents kinds of PCFs with chalcogenide core tellurite cladding composite microstructures. Compared with the large single-core PCF, the advantages of multi-core PCF are the higher nonlinearity coefficient and the larger effective mode area. We proposed that the multi-core PCF can support high-power light transmission and achieve high nonlinearity requirement. The small single-core PCF has a very high nonlinearity coefficient. At the wavelength $\lambda = 0.8$ μm, the nonlinearity coefficient can reach 31.37053 $W^{-1}\cdot m^{-1}$, and at the wavelength $\lambda = 1.55$ μm, the nonlinearity coefficient is 11.19686 $W^{-1}\cdot m^{-1}$.

References

[1] Xiao L, Zhang W, Huang Y D and Peng J D 2008 *Chin. Phys. B* **17** 995

[2] Wang W, Hou L T, Liu Z L and Zhou G Y 2009 *Chin. Phys. Lett.* **26** 114202

[3] Ebendorff-Heidepriem H, Petropoulos P, Asimakis S, Finazzi V, Moore R, Frampton K, Koizumi F, Richardson D and Monro T 2004 *Opt. Express* **12** 5082

[4] Ademgil H and Haxha S 2009 *Opt. Commun.* **282** 2831

[5] Razzak S M A and Namihira Y 2011 *Optik* **122** 1084

[6] Zhang C, Zhang Y Y, Hu M L, Wang S J, Song Y J, Chai L and Wang C Y 2012 *Opt. Commun.* **285** 2715

[7] Li P X, Zhang X X, Liu Z and Chi J J 2011 *Chin. Phys. Lett.* **28** 84206

[8] Limpert J, Schreiber T, Nolte S, Zellmer H, Tunnermann T, Iliew R, Lederer F, Broeng J, Vienne G, Petersson A and Jakobsen C 2003 *Opt. Express* **11** 818

[9] Chen M Y, Sun B, Zhang Y K, Tong Y Q and Zhou J 2010 *Opt. Commun.* **283** 3153

[10] Vogel M M, Abdou Ahmed M, Voss A and Graf T 2009 *Opt. Lett.* **34** 2876

[11] Chen G, Jiang Z W, Peng J G, Li H Q, Dai N L and Li J Y 2012 *Acta Phys. Sin.* **61** 144206 (in Chinese)

[12] Zhang X, Hu M L, Song Y L, Chai L and Wang Q Y 2010 *Acta Phys. Sin.* **59** 1863 (in Chinese)

[13] Husakou A 2003 *Appl. Phys. Lett.* **83** 3867

[14] Fang X H, Hu M L, Liu B W, Chai L, Wang Q Y and Zheltikov A M 2010 *Opt. Lett.* **35** 2326

[15] Fang X H, Hu M L, Song Y J, Xie C, Chai L, Wang Q Y 2011 *Acta Phys. Sin.* **60** 64208 (in Chinese)

[16] Manili G, Modotto D, Minoni U, Wabnitz S, Angelis C D, Town G, Tonello A and Couderc V 2011 *Opt. Fiber Technol.* **17** 160

[17] Imamura K, Tsuchida Y, Mukasa K, Sugizaki R, Saitoh K and Koshiba M 2011 *Opt. Express* **19** 10595

[18] Zheng Y B, Yao J Q, Zhang Lei, Wang Y, Wen W Q, Jing L and Di Z G 2012 *Chin. Phys. Lett.* **29** 24203

[19] Xie D and Wen J G 2011 *Adv. Mater. Res.* **308** 517

[20] Chaudhari C 2010 *Proc. SPIE* **7728** 772810

[21] Chaudhari C, Liao M, Suzuki T and Ohishi Y 2012 *J. Lightwave Technol.* **30**

[22] Liao M, Chaudhari C, Qin G, Yan X, Kito C, Suzuki T, Ohishi Y, Matsumoto M and Misumi T 2009 *Opt. Express* **17** 21608

[23] Liao M, Yan X, Qin G, Chaudhari C and Yasutake O T S 2010 *J. Non-Cryst. Solids* **356** 2613

[24] Lamont M R, Luther Davies B, Choi D Y, Madden S and Eggleton B J 2008 *Opt. Express* **16** 14938

[25] Zhou H S, Li S G, Fu B, Yao Y Y and Zhang L 2010 *Chin. Phys. Lett.* **27** 14208

[26] Cheng T L, Cai L, Hu M L, Li Y F and Wang Q Y 2010 *Chin. Phys. Lett.* **27** 114210

[27] Fang X H, Hu M L, Li Y F, Chai L and Wang Q Y 2011 *J. Lightwave Technol.* **29** 3428